Q. J. R. Meteorol. Soc. (2003), **129**, pp. 477–493 doi: 10.1256/qj.02.23

Relations between radar reflectivity, liquid-water content, and rainfall rate during the MAP SOP

By MARTIN HAGEN[1]* and SANDRA E. YUTER[2]

[1]*Institut für Physik der Atmosphäre, DLR, Oberpfaffenhofen, Germany*
[2]*University of Washington, Seattle, USA*

(Received 28 January 2002; revised 7 August 2002)

SUMMARY

Raindrop size distribution data obtained from two Joss–Waldvogel disdrometers located at Locarno-Monti, Switzerland during the Mesoscale Alpine Programme (MAP) Special Observation Period are analysed to obtain appropriate relationships of radar reflectivity, Z, with both water content, W, and surface rainfall, R, for use in MAP applications. The disdrometer data are accumulated into 10-minute samples to reduce sampling error associated with the $\sim$1 m^3 sample volume of the instruments. Based on previous studies, relations of the form $W = qZ^{(4/7)}$ and $Z = aR^{1.5}$ are assumed and the coefficients q and a are estimated from the data. The combined dataset of 10-minute samples from the two disdrometers and the 10-minute data divided into two independent subsets yielded similar mean values of the coefficients. The recommended relationships are $W = 3.4Z^{(4/7)}$ and $Z = 216R^{1.5}$. The uncertainties in these mean relationships as expressed in terms of ± 1 standard deviation are approximately equivalent to a ± 4.4 dBZ error for the Z–W relationship, and to a ± 2.4 dBZ error for the Z–R relationship.

KEYWORDS: Disdrometer Mesoscale Alpine Programme Radar meteorology Raindrop size distribution Sampling errors

1. INTRODUCTION

Maps of near-surface rainfall are important in understanding the water cycle of a region and in applications such as flood forecasting, fresh-water management, and detection of climate change. Scanning weather radars yield maps of radar reflectivity (Z) which can be used to estimate surface rainfall (R). The relationship between measured Z and R is complex and the estimation procedure is subject to several independent sources of error (Austin 1987; Joss and Lee 1995). The geometry of the radar beam leads to the radar's measurement of reflectivity to be made 100s to 1000s of m above the surface. Biases in the estimate of the near-surface reflectivity of rain can result from the following: vertical variation of reflectivity in the storm between the measurement several km above the surface and the surface; errors in radar calibration; non-meteorological echoes such a ground clutter and anomalous propagation; attenuation; and the presence of non-rain hydrometeors such as graupel, hail, and melting snow. These potential sources of bias can be removed or minimized by established methods†. For the purposes of this paper, we will assume that such procedures are utilized. We will focus on the relatively smaller magnitude biases in the mapping of Z to R (Joss and Lee 1995) associated with variations in the raindrop size distribution (RDSD).

An estimate of three-dimensional liquid-water content (W) of a storm volume can be obtained when radars scan several elevation angles to obtain a three-dimensional volume of radar reflectivity. In this context, the liquid-water content is more precisely a rain-water content since it does not include cloud drops to which the radar is insensitive. Volumetric liquid-water content derived from radar reflectivity can be useful in the initialization and validation of numerical models, and in studies utilizing aircraft *in situ* data. The Z–W estimation procedure has all the sources of error associated with the

* Corresponding author: Deutsches Zentrum für Luft- und Raumfahrt (DLR), Institut für Physik der Atmosphäre, Weßling, Germany. e-mail: martin.hagen@dlr.de

† See Joss and Lee (1995), Joss *et al*. (1998), Vignal *et al*. (2000), and Germann and Joss (2002) for detailed discussion of these methods as they are applied by MeteoSwiss to operational radar data.

estimation of R except for the vertical variation in Z since a transformation to near-surface values is not required.

During the Mesoscale Alpine Programme (MAP) Special Observing Period (SOP) (Bougeault *et al.* 2001), the RDSD within orographic precipitation was measured using two disdrometers deployed at the MeteoSwiss Osservatorio Ticinese in Locarno-Monti, Switzerland. These data are analysed to estimate appropriate Z–R and Z–W relations for the SOP.

2. Data

A disdrometer measures drop size distribution by counting the number of drops within each of several size categories over a time interval. We used two Joss–Waldvogel disdrometers (Joss and Waldvogel 1967; Waldvogel 1974), one operated by the Deutsches Zentrum für Luft- und Raumfahrt (DLR) Institut für Physik der Atmosphäre and one operated by the University of Washington (UW). The UW instrument is the standard RD-69/ADA-90 instrument. The DLR instrument combines the RD-69 and a custom built RDSD analyser. The Joss–Waldvogel disdrometer is an electro-mechanical instrument. The momentum of a raindrop falling at its terminal velocity on a styrofoam cone with area 50 cm^2 is converted to an electrical impulse. The amplitude of this impulse is proportional to the diameter of the raindrop. The instruments utilize 20 size categories to measure drops. Specific size categories are from $\sim$0.3 mm to $\sim$5 mm diameter for the UW disdrometer and $\sim$0.5 mm to $\sim$5 mm for the DLR disdrometer. Drops smaller than $\sim$0.3 mm do not produce an impulse sufficiently above the noise level. Larger raindrops are all grouped into the last of the 20 classes. The mean diameter of this 20th size category, which represents the drops larger than a particular size, has the largest uncertainty compared to the other 19 size categories which have both minimum and maximum diameter limits. The size categories for the DLR disdrometer were calibrated by measuring the transfer function of the signal-processing electronics (Sheppard 1990). The UW disdrometer used the factory calibration and standard diameter categories supplied by the instrument manufacturer, Distromet Inc.

At higher rainfall rates, the detection efficiency for small drops in the Joss–Waldvogel disdrometer is reduced compared to that at lower rainfall rates due to the generation of environmental noise by the rain itself. Environmental noise and man-made noise, when present, increase the noise level in the instrument below which drops cannot be detected (Joss and Gori 1976).

A short 'dead-time' is built into the instrument so that splashes associated with the impact of a large drop on the sensor are not counted as small drops within the RDSD. However, during this dead-time, neither splash products nor actual drops in the RDSD are measured. In order to account for the drops in the RDSD that were missed, a dead-time correction is applied which is a function of the number and size of drops counted by the instrument (Sheppard and Joe 1994). The main effect of the dead-time corrections is to increase the number of small drops within the distribution, since small drops are more numerous than larger drops and hence more likely to fall within the short dead-time period. The dead-time correction is designed to correct within $\pm$10% both for drops missed during the dead time of the instrument and for environmental noise due to rain (Joss and Gori 1976). The correction is not designed to account for missed drops due to an increase in the noise floor as a result of man-made noise, or for drops not hitting the instrument because of wind effects (Folland 1988).

As a data quality check, both disdrometers were compared to a nearby MeteoSwiss rain-gauge. Table 1 shows the daily rainfall accumulations computed from the

TABLE 1. DAILY SUMS OF PRECIPITATION MEASURED WITH THE RAIN-GAUGE AND TWO DISDROMETERS DLR AND UW

Date (1999)	Gauge (mm)	DLR (mm)	DLR within 10%	UW (mm)	UW within 10%
20 Sep	92.0	97.7	Y	43.8	incomplete
21 Sep	46.0	44.1	Y	42.8	Y
25 Sep	87.6	84.4	Y	88.4	Y
26 Sep	130.5	126.4	Y	73.2	incomplete
27 Sep	30.0	31.9	Y	30.9	Y
28 Sep	65.9	62.1	Y	62.0	Y
30 Sep	21.6	21.3	Y	21.7	Y
02 Oct	17.7	18.1	Y	19.0	Y
03 Oct	64.7	61.6	Y	61.7	Y
17 Oct	0.0	0.2		0.2	
18 Oct	0.6	0.8		0.8	
19 Oct	0.7	0.8		0.9	
20 Oct	13.6	13.0	Y	13.7	Y
21 Oct	53.9	50.0	Y	36.5	incomplete
22 Oct	6.2	4.8		7.1	
23 Oct	47.8	45.1	Y	46.7	Y
24 Oct	40.7	38.9	Y	42.5	Y
25 Oct	17.8	17.8	Y	18.6	Y
26 Oct	0.3	0.3	Y	0.3	Y
30 Oct	1.0	1.0	Y	1.1	Y
03 Nov	5.9	4.9		5.2	
04 Nov	29.2	26.4	Y	27.2	Y
05 Nov	1.2	1.3		1.3	Y
06 Nov	50.5	47.5	Y	49.8	Y
10 Nov	0.0	0.1		0.1	
11 Nov	8.1	17.9	Y	18.3	Y
14 Nov	6.8	6.5	Y	6.6	Y
15 Nov	2.9	2.9	Y	3.2	Y
17 Nov	8.0	7.9	Y	7.9	Y
18 Nov	0.7	0.0		0.0	
Total	861.9	835.6		731.2	
Total for complete days	585.5	561.5		577.8	

Y indicates days where the disdrometer is within 10% of the daily rainfall measured by rain-gauge. Totals are indicated for the full set of processed data obtained from each instrument and for the subset corresponding to the complete days for all three instruments.

MeteoSwiss rain-gauge and the two disdrometers. A total of 862 mm was recorded by the rain-gauge between 20 September and 19 November 1999. Overall, the instruments agreed well. Rain accumulations for both disdrometers were within 10% of the rain-gauge for all days with rainfall over 10 mm. For the four days with less than 1 mm rainfall measured by the disdrometers, the difference among the instruments was less than 0.2 mm. The measurement accuracy of the MeteoSwiss rain-gauge is 0.1 mm, corresponding to the rainfall associated with a single tip of this tipping-bucket type gauge. On 18 November 1999, the disdrometer-observed rain rates never exceeded 0.2 mm h^{-1} so these data were removed from the processed dataset (section 3(d)). The discrepancies among the instruments on 22 October and 3 November are still under investigation, but are likely to have some contribution from the 0.2 mm h^{-1} rain-rate threshold applied to the disdrometer data. The incomplete records from the UW disdrometer were the result of a computer rather than an instrument problem.

3. METHODOLOGY

The analysis of RDSD data collected by disdrometer must take into account the degree of representivity of the measurements in terms of their location and scale, and address statistical sampling error.

(*a*) *Representivity of location*

Locarno-Monti was within the Laggio-Maggiore Target Area (LMTA) of focused observations designed to address the precipitation-related objectives of MAP (Bougeault *et al.* 2001) and is near a climatological local maximum of heavy precipitation in the southern Alps (Frei and Schär 1998). Locarno-Monti received 30 days of rainfall during the period 20 September to 18 November 1999 within a variety of synoptic conditions (Bougeault *et al.* 2001), and was near the centre of the maximum rainfall accumulation during the MAP Intensive Observation Period (IOP) 2b event on 19–20 September 1999 (Rotunno and Ferretti 2003). The details of the rainfall distribution varied within the LMTA, so one location cannot be exactly representative of other locations within the LMTA or of the LMTA area mean.

(*b*) *Representivity of spatial-scale*

The spatial-scale of the recorded 1-minute disdrometer measurements is order 1 m^3. The spatial-scale of the radar measurements to which they are intended to be applied is $\sim$1 km^3. The order 10^9 difference in spatial-scales is staggeringly large. It would take over 1902 years for a single disdrometer to measure a volume of atmosphere equivalent to a typical individual radar-resolution volume. To date, all *in situ* measurements of the RDSD via either aircraft particle probes or surface-based disdrometers have had a sampling volume of 10 m^3 or less. Without instantaneous *in situ* observations at larger scales, it has been difficult to assess how well the variability of the RDSD in time represents its variability in space or how well averaging in time represents averaging in space.

Joss and Gori (1978) examined the characteristics of the RDSD over increasing time periods within two storms at Locarno-Monti, and found that after several hundred minutes the characteristics of the RDSD tended to converge toward an exponential distribution. A single instrument sample over 100s of minutes in duration is obtained within several different portions of the storm, and is possibly a result of several different precipitation processes. Joss and Gori (1978) recognized this limitation. They concluded that 'true exponential distributions are obtained when adding many 1-minute samples of different rain intensity'. They also found that the rate of change of the RDSD shape was not constant but varied approximately with the natural logarithm of the accumulation time. For example, the relative difference in average shape of the RDSD between samples for 1- and 10-minute accumulations was larger than between samples for 11- and 20-minute accumulations. In their examination of the degree of uniformity of precipitation processes, Kostinski and Jameson (1997) analysed disdrometer time series data and found $\sim$10-minute duration rain 'patches' with a similar number of drops of a given size per minute. They described the RDSD at larger scales that would incorporate multiple rain 'patches' as mixtures of Poisson distributions (Jameson and Kostinski 2001).

(*c*) *Sampling error*

Smith *et al.* (1993) modelled sampling errors in a normalized exponential RDSD as a means to assess the relative contributions of sampling uncertainties versus natural

inhomogenities to the apparent variability of *in situ* RDSD measurements. They found a consistent low bias in estimates of R and Z that decreased as the total number of drops in the sample increased. The low bias is a result of the mismatch between the typical measurement sample volume of 1 m^3 and the average concentration of larger drops in the sample which is often less than 1 per m^3. For example, for an average concentration of 4 mm diameter drops of 1 drop per 100 m^3, on average 99 of 100 1-minute samples will not register a drop 4 mm in size . Without the large drop, the 99 samples will have a low bias in R and a slightly larger low bias in Z because of the $\sim D^4$ compared to D^6 weighting. The one sample with the 4 mm drop will have high biases in R and Z, but when averaged with the other 99 samples the mean bias will be still be low. This type of sampling bias associated with an exponential-type distribution, where significant contributions to R and Z can come from low concentrations of large drops, is in addition to the Poisson uncertainty which is based on the number of drops measured.

(*d*) *Processing procedure*

To process the disdrometer data to reduce uncertainties we have to compromise between two conflicting constraints. To reduce sampling error we should increase the number of drops by increasing the sampling accumulation time. To reduce errors associated with mixing samples representing distinct precipitation processes, we should keep the sampling time small. As a compromise between these two constraints, we have chosen a 10-minute accumulated RDSD as the basis of our analysis, and a 60-minute accumulated RDSD for comparison. A 10-minute accumulation period allows us to reduce but not eliminate sampling errors. A 60-minute accumulation period permits us to reduce sampling error further but at the expense of mixing rain patches. Since we are comparing data obtained from two instruments, we have the additional constraint that we would like to compare the same time periods, e.g. 01:00:00–01:09:59. This latter constraint means that sometimes we will include minutes within the 10-minute period where an individual instrument did not measure any drops*. A time period is considered rainy if at least 80% of the 1-minute measurements within the period had drops. In processing the data, we have removed 1-minute measurements with less than 20 raw drop-counts (not dead-time corrected) which usually correspond to non-precipitation triggers such as wind hits and insects. We have also applied a minimum rain-rate threshold of 0.2 mm h^{-1} to remove accumulated samples prone to large sampling errors.

Radar reflectivity (assuming Rayleigh scattering), liquid-water content and rain rate were calculated from the dead-time corrected RDSD ($N(D)$ with N the number of drops and D the drop diameter, in units of $m^{-3}mm^{-1}$) as follows.

$$Z = \sum_{i=1}^{20} N(D_i) D_i^6 \Delta D_i, \tag{1}$$

$$W = \frac{\pi}{6} \sum_{i=1}^{20} N(D_i) D_i^3 \Delta D_i, \tag{2}$$

$$R = \frac{3.6\pi}{6000} \sum_{i=1}^{20} N(D_i) D_i^3 V(D_i, T, P) \Delta D_i. \tag{3}$$

* This processing method differs from other methods where consecutive rainy minutes are processed into 10-minute accumulated samples.

TABLE 2. RAINDROP SIZE DISTRIBUTION DATA SAMPLE STATISTICS

Sample description	Rain-rate category (mm)	Number of samples	Total accumulation (mm)	Average rain rate (mm h^{-1})	Drop counts per sample (as measured; no dead-time correction) Min.	Mean	Max.
(a) For full 10-minute and 60-minute datasets for disdrometers DLR and UW							
DLR 10-minute	All	1432	835	3.5	116	3445	12 601
	$R < 1$	504	44	0.5	116	1735	6998
	$1 \leqslant R < 5$	674	265	2.4	255	3912	12 601
	$5 \leqslant R$ 10	138	157	6.8	1425	5147	10 502
	$10 \leqslant R < 50$	112	326	17.5	1192	6088	9580
	$R \geqslant 50$	4	43	64	7140	7658	8120
UW 10-minute	All	1310	731	3.3	128	4075	17 566
	$R < 1$	487	43	0.5	128	2238	9828
	$1 \leqslant R < 5$	607	244	2.4	315	4561	17 555
	$5 \leqslant R$ 10	113	131	6.9	1533	6245	12 068
	$10 \leqslant R < 50$	100	286	17.1	2485	7431	11 228
	$R \geqslant 50$	3	28	56.1	9662	10 158	10 905
DLR 60-minute	All	269	831	3.1	735	18 306	61 638
	$R < 1$	82	42	0.5	735	8818	29 364
	$1 \leqslant R < 5$	144	334	2.3	2883	20 674	61 638
	$5 \leqslant R < 10$	25	174	7	6298	23 445	46 477
	$10 \leqslant R < 50$	18	281	15.6	17 018	35 447	49 893
	$R \geqslant 50$	0	–	–	–	–	–
UW 60-minute	All	245	729	3.0	1930	21 807	96 483
	$R < 1$	80	40	0.5	1930	12 053	44 142
	$1 \leqslant R < 5$	127	297	2.3	6299	23 641	96 483
	$5 \leqslant R < 10$	22	145	6.6	11 150	31 235	55 131
	$10 \leqslant R < 50$	16	247	15.5	23 127	43 048	62 608
	$R \geqslant 50$	0	–	–	–	–	–
(b) As (a) except for *timeA10* and *timeB10* subsets of *combo10*							
timeA10	All	1370	1113	4.9	116	3817	14 141
	$R < 1$	412	36	0.5	116	2008	9828
	$1 \leqslant R < 5$	583	239	2.5	255	3697	14 141
	$5 \leqslant R < 10$	174	202	7	1425	5224	12 068
	$10 \leqslant R < 50$	194	565	17.5	1192	6579	11 114
	$R \geqslant 50$	7	71	60.6	7140	8729	10 905
timeB10	All	1370	452	2.0	119	3679	17 566
	$R < 1$	577	50	0.5	119	1966	8372
	$1 \leqslant R < 5$	698	270	2.3	612	4656	17 566
	$5 \leqslant R < 10$	77	85	6.6	2122	6584	11 457
	$10 \leqslant R < 50$	18	47	15.6	3874	8257	11 228
	$R \geqslant 50$	–	–	–	–	–	–

The total accumulation and average rain rates are calculated after the dead-time correction is applied. The UW data had sporadic dropouts due to a computer problem so the time periods of the DLR and UW data do not match exactly and, as a result, the statistics for the full datasets are not expected to match. The full DLR and UW 10-minute datasets are combined to yield the *combo10* dataset, and the 60-minute data are also combined to yield the *combo60* dataset. See text for further details.

For each of the 20 size categories, D_i is the mean diameter of the size category in mm, and ΔD_i is the width of the size category in mm. The units are: for Z, $mm^6 m^{-3}$; for W, $mm^3 m^{-3}$; and for R, mm h^{-1}. The particle fall speed, V, is a function of diameter, temperature, T, and pressure, P (Berry and Pranger 1974) and is in units of m s^{-1}.

For our analysis we used several versions of the disdrometer data, the union of the 10-minute accumulated DLR and UW data, *combo10*, and the union of the 60-minute accumulated DLR and UW data, *combo60*. Table 2(a) shows statistics for the full DLR and UW 10-minute and 60-minute datasets separately. Additionally, two independent subsets, *timeA10* and *timeB10,* were obtained by dividing the *combo10* data by time

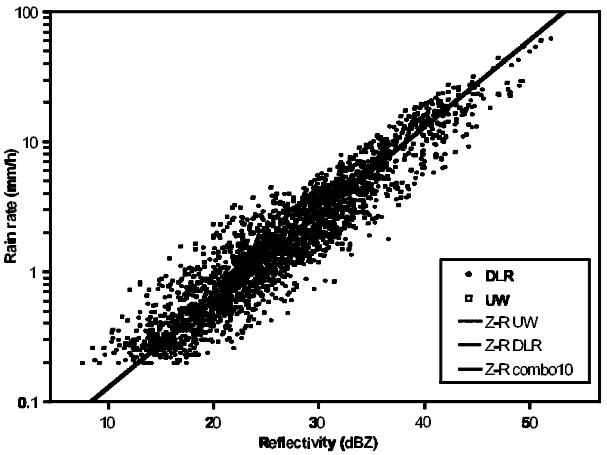

Figure 1. Plot of calculated reflectivity, Z, versus calculated rainfall rate, R, from 10-minute accumulated DLR and UW disdrometer raindrop size samples. Z–R relations are indicated based on mean coefficient a values for: *combo10* dataset, $Z = 216R^{1.5}$ (solid line); *DLRoverlap10* subset of $Z = 219R^{1.5}$ (dotted line); and *UWoverlap10* subset of $Z = 205R^{1.5}$ (dashed line). See text for details.

(before and after 2230 UTC 22 October 1999) to yield datasets each with 1370 samples (Table 2(b)). Although the time periods for *timeA10* and *timeB10* are identical in length, the precipitation was not distributed evenly through the SOP, and *timeA10* had a total rainfall accumulation of 1113 mm compared to the 452 mm of *timeB10* (Table 2(b)). By definition the sum (within round-off error) of the rainfall accumulations for *timeA10* and *timeB10* is equal to the sum of the rainfall accumulations for the DLR and UW 10-minute datasets (i.e. *combo10*). The effect of the dead-time of the instrument is evident in the smaller number of drops counted at higher rain rates. At least half of the rain accumulation was obtained within rain rates <10 mm h^{-1}. The 60-minute data have similar total accumulations but lower average rain rates compared to the 10-minute data, as is expected given the roughly log-normal distribution of 1-minute rain rates (Table 2(a)).

4. Analysis

(*a*) *Characteristics of samples from the two disdrometers*

The calculated Z versus calculated R values for the accumulated 10-minute samples from both disdrometers are shown in Fig. 1. The points from both disdrometers are scattered relatively evenly throughout the plot, indicating that the data from the two disdrometers probably represent two different samples from the same parent population. Overall there is a large scatter of up to 10 dBZ for a given rain rate, with some portion of the scatter related to sampling error associated with the small sample volumes (section 2(c)) and the remaining portion due to natural variability.

To determine if the DLR and UW datasets have a relative bias between the two instruments, the subset of data from each instrument corresponding to the time when both instruments recorded rainfall was examined, *DLRoverlap10* and *UWoverlap10*, corresponding to 1243 10-minute samples from each. The frequency distributions of Z and $\log_{10}(R)$ (Figs. 2 and 3) are very similar overall as are the statistics in Table 3. Given sampling errors and the small spatial-scale variability of rainfall (Habib and Krajewski 2002) we do not expect instruments a few metres apart to obtain identical samples.

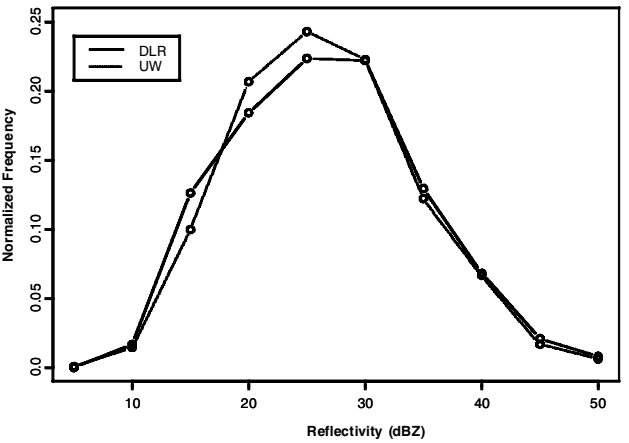

Figure 2. Normalized frequency distribution of calculated reflectivity, Z, values for *DLRoverlap10* and *UWoverlap10* (dotted line) corresponding to 10-minute accumulations during the subset of observation periods when both DLR and UW distrometers recorded rain rates > 0.2 mm h^{-1}. See text for details.

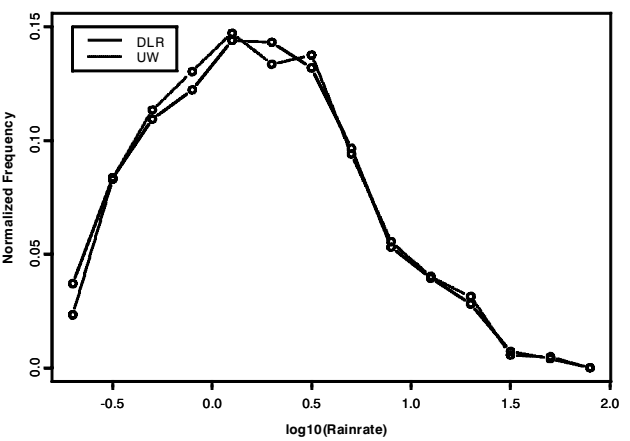

Figure 3. Same as Fig. 2 but for calculated rainfall, R, values.

The difference in rainfall accumulation between the two instruments is less than 2% (Table 3). While there are slight differences between the DLR and UW subsets, there is no significant relative bias between them. We conclude that it is reasonable to combine the data from both instruments in our analysis.

(*b*) *Calculation of Z–W and Z–R relations*

The methods of calculating Z–R and Z–W relations from measured RDSD are almost as numerous as the number of papers that treat this subject. The resulting relationship can be very sensitive not only to the input data but also to the method by which it was calculated (Campos and Zawadzki 2000).

(i) Z–W. For the Z–W relations, we use a quadratic equation of the form $W = qZ^{4/7}$ (Kessler 1969; Smith et al. 1975) which simplifies into the linear equation:

$$\log_{10}(W) = \log_{10}(q) + (4/7)\log_{10}(Z). \tag{4}$$

TABLE 3. COMPARISON OF STATISTICS BETWEEN DISDROMETERS DLR AND UW 10-MINUTE ACCUMULATIONS DURING THE 207.2 h WHEN BOTH RECORDED RAIN RATES > 0.2 mm h^{-1}

	Statistic	*DLRoverlap10*	*UWoverlap10*
Rain rate (mm h^{-1})	Min.	0.2	0.2
	1st Quartile	0.7	0.7
	Median	1.6	1.6
	Mean	3.4	3.5
	Standard deviation	5.5	5.5
	3rd Quartile	3.7	3.8
	Max.	61.8	60.5
Rain	Accumulation (mm)	710	723
Reflectivity (dBZ)	Min.	7.5	8.7
	1st Quartile	21.1	20.8
	Median	26.3	26.4
	Mean	26.7	26.8
	Standard deviation	8.0	7.6
	3rd Quartile	31.6	32.1
	Max.	51.1	52.1

The exponent 4/7 in the Z–W relation is obtained as follows. The RDSD is approximated as an exponential distribution, $N(D) = N_o\, e^{-\Lambda D}\, dD$ for D from 0 to infinity where N_o is a constant. The definite integral forms of (1) and (2) are integrated and applied to the general formula $W = qZ^s$ to obtain:

$$\frac{N_o \pi !}{\Lambda^4} = q\left(N_o \frac{6!}{\Lambda^7}\right)^s. \tag{5}$$

Setting $s = 4/7$ will cancel the Λ terms and remove the direct dependency of q on W. Following the methodology of Doelling *et al.* (1998) for determining Z–R, we determine a value of q for each sample of the population using $q = W/(Z^{4/7})$.

The plot of $\log_{10}(q)$ versus $\log_{10}(W)$ (Fig. 4(a)) illustrates that $\log_{10}(q)$ values are uncorrelated with W and vary between approximately 0.3 and 30 q units. The sloping lower edge of the cloud of points is an artifact of the thresholding of the processed data on a 0.2 mm h^{-1} rain rate. Lines of constant rain rate are roughly parallel to the lower-right edge. The narrower distribution of q values for higher rain rates is expected, since the higher rain-rate samples have a larger number of drops and less statistical sampling error than the lighter rain-rate samples (see section 3 and Table 2). The distribution of q is approximately log-normal (Fig. 4(b)) and the distribution of $\log_{10}(q)$ for this dataset is close to Gaussian (Fig. 4(c)). A Gaussian distribution of $\log_{10}(q)$ is not generally true, especially for smaller sample sizes. We use the mean* $\log_{10}(q)$ value to obtain the best estimate, and ± 1 standard deviation (σ) of $\log_{10}(q)$ as an assessment of the uncertainty (Table 4). The bottom half of Table 4 shows the equivalent values in q units. Since ± 1 standard deviation of $\log_{10}(q)$ is not symmetric in q, we have indicated $-\sigma$ as the 16th percentile and $+\sigma$ as the 84th percentile. Figure 4(d) and the biases in Table 4 provide information on how well (4) estimates liquid-water content from Z compared to liquid-water content calculated from the RDSD in (2). Cumulative bias is:

$$\Sigma\ estimated / \Sigma\ calculated,$$

and average bias is:

$$\Sigma(estimated/calculated)/N.$$

* Doelling *et al.* (1998) used the median rather than the mean of $\log_{10}(q)$.

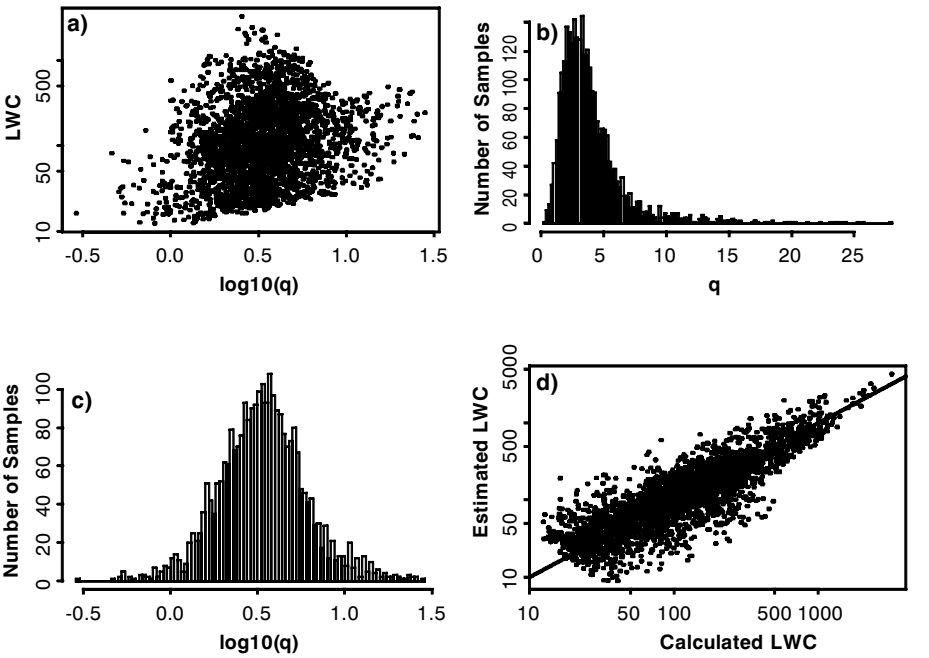

Figure 4. Plots of: (a) raindrop size distribution (RDSD) calculated liquid-water content, W, versus coefficient q in $W = qZ^{(4/7)}$, where Z is radar reflectivity; (b) frequency distribution of q; (c) frequency distribution of $\log_{10}(q)$; and (d) Plot of RDSD-calculated W versus estimated W using $W = 3.4Z^{(4/7)}$ and calculated Z. Plots are based on the *combo10* dataset (see text).

TABLE 4. ESTIMATES OF COEFFICIENT q AND ITS UNCERTAINTIES AND BIASES IN $\log_{10}(W) = \log_{10}(q) + (4/7)\log_{10}(Z)$ AND $W = qZ^{4/7}$

		combo10	*combo60*	*timeA10*	*timeB10*
log10(q)	mean	0.529	0.460	0.517	0.540
	σ	0.25	0.23	0.25	0.26
	median	0.527	0.458	0.536	0.517
	r^2	1.05	1.09	1.09	0.97
	cumulative bias	1.00	1.0	1.0	1.0
	average bias	1.01	1.01	1.01	1.01
q	mean	3.4	2.9	3.3	3.5
	16th percentile	1.9	1.7	1.9	1.9
	84th percentile	6	4.9	5.8	6.2
	r^2	1.05	1.09	1.09	0.97
	cumulative bias	1.05	1.05	1.07	0.99
	average bias	1.18	1.16	1.19	1.18

σ is the standard deviation, r^2 is the ratio of explained variation to total variation (coefficient of determination). See text for further details.

While the spread of points around the 1:1 line in Fig. 4(d) is wide, there is no bias to the cumulative estimate based on (4). Individual estimates of W for dependent data will have an average positive bias of 15–18%. The difference in the mean values between the *combo10* and *combo60* data is larger than the standard error of the mean ($\sigma/\sqrt{N}$), but its physical significance is difficult to assess. The shift in the *combo60* mean value of q toward lower values is consistent with a reduction in the low bias of calculated Z relative to W associated with a smaller sampling error. The *combo60* dataset has the

positive aspect of having a smaller sampling error in each sample, but it has the negative aspects of a smaller total number of samples and larger errors associated with mixing rain patches compared to *combo10*. Also, short-duration rain events lasting less than 48 minutes in a given hour are not included in the *combo60* dataset. A much larger dataset than that obtained during MAP would be needed to be able to quantify the relative contributions of these sources of uncertainty to the difference in mean q between the *combo10* and *combo60* datasets.

(ii) Z–R. Calculation of rain-rate requires knowledge of particle fall speed $V(D, T, P)$ (see (3)). For surface-based disdrometer data, the vertical air velocity is assumed to be zero, and T and P are treated as constants (here we use $T = 20\,^{\circ}\mathrm{C}$, $P =$ 1013.25 hPa). For radar measurements and *in situ* data obtained by aircraft these physical assumptions are not valid, and can lead to errors in estimated fall speed and hence rain rate (Dotzek and Beheng 2001). We cannot parallel the methodology used to obtain an equation for Z–W, as expressions for fall speed (Berry and Pranger 1974) that closely match empirical data do not have a simple functional form amenable to a definite integral solution for R. For the Z–R relation* we assume a quadratic equation of the form $Z = aR^{1.5}$, which simplifies to the linear equation:

$$\log_{10}(Z) = \log_{10}(a) + (1.5)\log_{10}(R). \tag{6}$$

The fixed exponent of 1.5 for the Z–R relation was originally proposed by Smith and Joss (1997) based on empirical studies, and has been tested with multi-year samples of disdrometer data by Doelling *et al.* (1998) and Steiner and Smith (2000).

The values of the coefficient a as a function of rain rate for each of the 10-minute samples in *combo10* are shown in Fig. 5(a). If there were distinct a values for lighter versus heavier precipitation, it would manifest in the scatter plot as discernably different populations of points as a function of R. Instead, we have one widely scattered population of a values centred roughly between $\log_{10}(a)$ values of 2 to 2.7. As in Fig. 4(a), there is a narrower distribution of a values for higher rain rates, >5 mm h^{-1} compared to <5 mm h^{-1}, since the higher rain-rate samples have less statistical sampling error.

The distribution of a is approximately log-normal (Fig. 5(b)), similar to the characteristics of the distribution of q (Fig. 4(b)), while $\log_{10}(a)$ is roughly normal (Fig. 5(c)).

Similar to the procedure used to obtain the Z–W relationship, we compute the mean value and standard deviation of $\log_{10}(a)$ and their equivalent values in a (Table 5). The resulting relationships are $Z = 216R^{1.5}$ for *combo10* (Fig. 1) and $Z = 268R^{1.5}$ for *combo60*. Again, the statistics for the *combo60* data are shifted toward higher a values, which is consistent with a reduction in the low bias of calculated Z relative to calculated R associated with a smaller sampling error. The fall velocity factor in R is likely to have a compensating effect for some types of errors, as the biases in Table 5 are slightly smaller than in Table 4 such that an individual estimate of R for dependent data will have an average positive bias of $\sim$10%.

The mean $\log_{10}(a)$ Z–R relations for the overlapping time period of the two disdrometers are $Z = 219R^{1.5}$ for *DLRoverlap10*, and $Z = 205R^{1.5}$ for *UWoverlap10* (Fig. 1). Linear regression of these two datasets results in Z–R relations of $Z =$

* Although we are interested in obtaining a relation to transform observed Z into estimated R, and use Z as the independent variable in our computations, we will follow the convention of describing this relation in terms of $Z = aR^b$ so that our results can be more readily compared to those reported by other investigators.

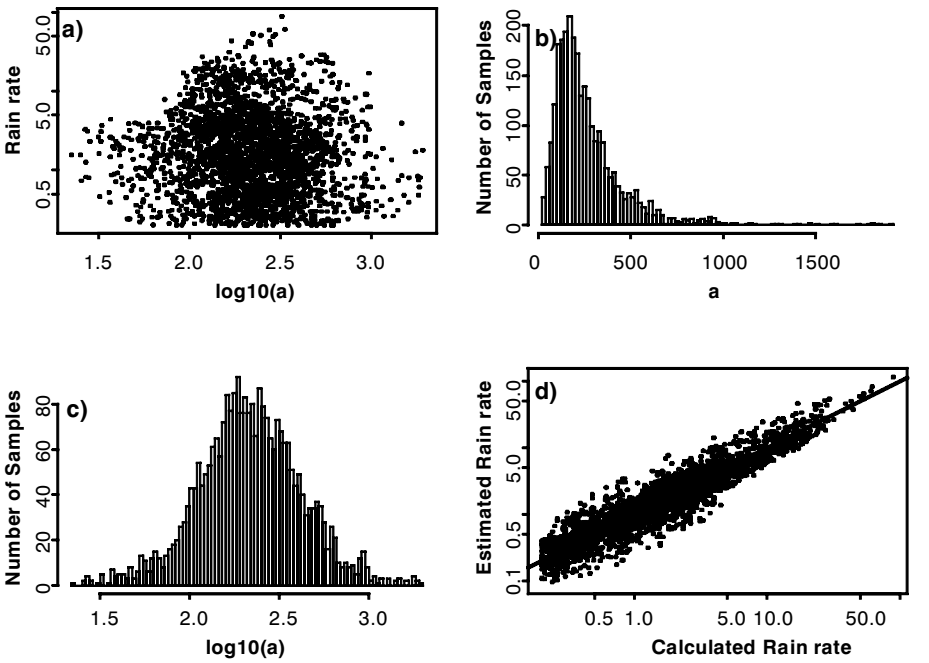

Figure 5. Plots of: (a) raindrop size distribution (RDSD) calculated rain rate, R, versus coefficient a in $Z = aR^{(1.5)}$, where Z is radar reflectivity; (b) frequency distribution of a; (c) frequency distribution of $\log_{10}(a)$; and (d) Plot of RDSD-calculated R versus estimated R using $Z = 216R^{1.5}$ and calculated Z. Plots are based on the *combo10* dataset (see text).

TABLE 5. ESTIMATES OF COEFFICIENT a AND ITS UNCERTAINTIES AND BIASES IN $\log_{10}(Z) = \log_{10}(a) + (1.5)\log_{10}(R)$ AND $Z = aR^{1.5}$

		combo10	*combo60*	*timeA10*	*timeB10*
log10(a)	mean	2.335	2.428	2.340	2.332
	σ	0.29	0.27	0.29	0.29
	median	2.332	2.427	2.309	2.355
	r^2	1.09	1.11	1.1	1.08
	cumulative bias	1.0	1.0	1.0	0.99
	average bias	1.0	0.89	0.98	1.01
a	mean	216	268	219	215
	16th percentile	112	144	113	111
	84th percentile	418	499	424	417
	r^2	1.09	1.11	1.10	1.08
	cumulative bias	1.07	1.06	1.08	1.03
	average bias	1.1	1.09	1.11	1.09

σ is the standard deviation, r^2 is the ratio of explained variation to total variation (coefficient of determination). Values of $\log_{10}(R) = 0$ are removed from the dataset in the calculation of average bias. See text for further details.

$221R^{1.48}$ (*DLRoverlap10*), and $Z = 214R^{1.42}$ (*UWoverlap10*). Therefore, for the disdrometer data obtained during the SOP the assumption of 1.5 as the exponent in the Z–R relation is reasonable.

Another method of estimating the a value is to use its rain-rate-weighted median rather than its arithmetic mean. Samples contributing more to the rainfall accumulation are given heavier weighting, yielding an estimate of a which will have smaller errors

TABLE 6. IMPACT OF ± STANDARD DEVIATION IN COEFFICIENT q IN $W = qR^{4/7}$ COMPARED TO *combo10* MEAN VALUE OF 3.4

Value of coefficient q	1.9	3.4	6
% difference in W estimated from Z	56%	100%	176%
Difference in dBZ estimated from W	−4.4	0	4.3

See text for details.

TABLE 7. IMPACT OF ± STANDARD DEVIATION IN COEFFICIENT a IN $Z = aR^{1.5}$ COMPARED TO *combo10* MEAN VALUE OF 216

Value of coefficient a	112	216	418
% difference in R estimated from Z	155%	100%	64%
Difference in dBZ estimated from R	2.3	0	−2.4

See text for details.

when used in applications to estimate rainfall accumulations, but larger errors in applications to estimate individual rain rates. To estimate the best rain-rate-weighted a value, the distribution of $\log_{10}(a)$ is sorted by increasing rain rate and the median value determined. This rain-rate-weighted median method yields $Z = 215R^{1.5}$ for *combo10*, which is nearly identical to the arithmetic mean value of $Z = 216R^{1.5}$ for the non-weighted data (Table 5). For the *combo60* data, the rain-rate-weighted median method yields $Z = 255R^{1.5}$. The difference between this and the non-weighted mean relations ($Z = 268R^{1.5}$ from Table 5) corresponds to only a 0.2 dBZ difference for a given R.

(*c*) *Uncertainties and their impact*

A recommendation to use a particular Z–W or Z–R relation is not truly complete without information on how well the suggested relations perform on independent data. The nature of errors associated with these relations makes sample size particularly important, and it is not uncommon for the entire available dataset to be used to estimate the Z–W or Z–R relation even in multi-year datasets (e.g. Doelling et al. 1998; Steiner and Smith 2000). The quality of the relation may be lowered if the sample size is reduced below some critical value. Unfortunately, having used all the data to obtain our best estimate we have no independent data with which to test it.

We address the uncertainty associated with our methodology by examining two independent datasets (*timeA10* and *timeB10*) based on storms sampled before and after 2230 UTC 22 October 1999 at Locarno-Monti. This calculation is equivalent to assuming that the rainy portion of the SOP was half as long, and applying the Z–W and Z–R relations obtained in one half to the independent data collected in the other half. The mean coefficients vary slightly for Z–W (Table 4) and for Z–R (Table 5) compared to the *combo10* dataset as a whole. Application of the relations derived for one half of the data to the Z data obtained in the other half yields cumulative biases of net liquid-water content and rainfall of 94% and 113% for the Z–W relations and 101% and 110% for the Z–R relations.

By definition, 68.27% of the samples in the population fall within $\pm\sigma$. The impact of applying the relations corresponding to the $\pm\sigma$ q and a values are shown in Tables 6 and 7. For comparison, the typical error in R associated with not correcting for the variation of the profile of reflectivity between the lowest radar measurement and the ground is 3 dB (factor of two) in the Alps (Germann and Joss 2002).

5. Conclusions

RDSD data obtained from two Joss–Waldvogel disdrometers deployed at Locarno-Monti during MAP were analysed to yield recommended Z–W and Z–R relations and their uncertainties. Disdrometer data were accumulated into 10-minute and 60-minute samples to reduce, but not eliminate, sampling errors which usually manifest as a low bias in R and a lower bias in Z (Smith *et al.* 1993).

For the majority of radar data obtained during MAP without dual polarization, Z–W and Z–R relations provide a method to estimate volumetric liquid-water content and rain rate from observed radar reflectivity. Despite the large uncertainties, the recommended relations may be useful to map radar reflectivity into a form that can be qualitatively compared to other estimates of liquid-water content and rain rate. An advantage of the Z–W and Z–R relationships over dual-polarization methods (Bringi and Chandrasekar 2001) is that they can be applied to radar echo regions where the reflectivities are weak and the dual-polarization signal is noisy. A disadvantage of Z–W and Z–R methods is that they can yield large errors when they are mistakenly applied to regions which contain hydrometeors other than rain (e.g. the melting layer or regions containing snow, hail, or graupel). Large errors can also result when these relations are applied to reflectivities which have not been corrected for common sources of bias (section 1).

Empirical relations between radar reflectivity and liquid-water content do not appear frequently in the literature, despite their utility for comparison with aircraft *in situ* data and numerical model output and their relative simplicity compared to a Z–R relation. Our recommended relationship of $W = 3.4Z^{(4/7)}$ is valid for the raindrop portion of the liquid-water content where the drops are >0.2 mm diameter. Battan (1973) ennumerates 69 Z–R relations but only one Z–W relation for rain, $W = 3.9Z^{0.55}$ reported by Douglas (1964). Sekhon and Srivastava (1971) report a Z–W relation of $W = 0.98Z^{0.70}$ obtained from raindrop spectra inferred from vertically pointing Doppler radar measurements in a thunderstorm. Raindrop spectra derived from vertically pointing Doppler radar data are subject to spectral broadening from turbulence (Joss and Dyer 1972) so Sekhon and Srivastava's Z–W relation is not directly comparable to one obtained from *in situ* data.

The combined 10-minute accumulation (*combo10*) disdrometer dataset mean relation of $Z = 216R^{1.5}$ is bracketed by a lower bound of $Z = 112R^{1.5}$ and an upper bound of $Z = 418R^{1.5}$. These bounds encompass the 60-minute accumulation (*combo60*) mean relationship and all the Z–R relations used by the national weather services within the MAP SOP domain: Austria, France, and Italy, $Z = 200R^{1.6}$ (Marshall and Palmer 1948); Germany, $Z = 256R^{1.42}$ (Aniol *et al.* 1980); and Switzerland, $Z = 316R^{1.5}$ (Joss *et al.* 1998). A 5 dBZ difference will translate into a 105%, 125%, 115%, and 115% difference in R for the Marshall and Palmer (1948), Anoil *et al.* (1980), Joss *et al.* (1998) and MAP Z–R relations respectively.

The maximum difference in the mean coefficients in the Z–R relation, of 215 to 268, corresponds to only slightly more than 1 dBZ difference (Table 5). Errors in 30-day rainfall accumulation due to mean RDSD variations in independent data are within 10% (Table 5), while uncertainty based on $\pm\sigma$ in individual rain rates can be 64–155% (Table 7). The uncertainty in the Z–W relation in terms of $\pm\sigma$ (Table 6) is larger (56–176%) than in the Z–R relation. Although uncomfortably large for some applications, the relative sizes of these errors are smaller or comparable to several other known error sources in rainfall mapping from radar data, and emphasize the importance of correcting overall biases with proper radar calibration and biases as a function of range using procedures to account for the variations in the vertical profile of precipitation from the

height of radar measurement to the ground (Joss and Lee 1995, Dotzek and Beheng 2001, Germann and Joss 2002).

Our recommended Z–W and Z–R relationships for the LMTA would be slightly different if the disdrometer data had been obtained at a location within the LMTA other than Locarno-Monti, or if the SOP had been scheduled to start a few days later, a few days earlier, or in a different year. Differences in data processing, whether a mean, median value, or weighted median is used as the population estimate, and which subsets of the data are examined, can yield variations in values of the coefficients in the Z–W and Z–R relations with little physical significance (Tables 3, 4, and 5). Our goal was to obtain a relation that will work well on average for data obtained within the LMTA during the SOP. We did not produce relations for each IOP, since these would only have value if we could also show that the relationship between rainfall at Locarno-Monti compared to other areas within the LMTA was similar among IOPs. Rainfall maps derived from rain-gauge data show large variability in the spatial distribution of rainfall in the LMTA among IOPs so this is unlikely to be the case.

If there were a strong relation between the coefficient values in the Z–W and Z–R relations and distinct precipitation processes, such as precipitation growth by accretion of cloud liquid water versus growth by vapour deposition, these would manifest as discernably distinct populations in the scatter plots in Figs. 4(a) and 5(a). In particular one would expect a distinction between heavy rain $>\sim$10 mm hr^{-1}, which is primarily a result of accretional processes, and lighter rain which can be a result of a variety of precipitation processes. When the *combo10* data are divided into subsets corresponding to samples with rain rates $>$10 mm hr^{-1} and $\leqslant$10 mm hr^{-1}, the mean coefficients for the Z–R relation are 219 and 216, respectively. The absence of distinct populations in the scatter plots indicates that either different precipitation processes occurring at Locarno-Monti during MAP do not have strong and distinctly different signals in the coefficients of Z–W and Z–R, or that one precipitation process dominates the samples in both heavier and lighter rain.

Since it is unlikely that variations in RDSD follow national boundaries, it would be useful to create a merged rainfall product based on quality controlled radar data for the MAP domain using a single Z–R relationship. From a qualitative standpoint, the exact relation used is not critical, as all the national weather service relations are within one standard deviation of the recommended MAP relation. As errors in rain rate at a particular point estimated from radar data can be large (Fig. 5(d) and Table 7), comparisons between radar-derived rainfall and other datasets and numerical models are best carried out using areal averages or storm accumulations.

Acknowledgements

The authors gratefully acknowledge the collaboration of Jürg Joss and Urs Germann of the MeteoSwiss in the collection and analysis of the DLR and UW disdrometer data at Locarno-Monti. The second author also thanks MAP Principal Investigator Robert A. Houze, Jr. for his support and encouragement. The work of the second author was supported by NSF grant ATM-9817700 and NASA TRMM grant NAG5-9750.

References

Aniol, R., Riedl, J. and Dieringer, M. 1980 Über kleinräumige und zeitliche Variationen der Niederschlagsintensität. *Meteorol. Rdsch.*, **33,** 50–56

Austin, P. M. 1987 Relation between measured radar reflectivity and surface rainfall. *Mon. Weather Rev.*, **115,** 1053–1070

Battan, L. J. 1973 *Radar observation of the atmosphere*. University of Chicago Press, Chicago, USA

Berry, E. X. and Pranger, M. R. 1974 Equations for calculating the terminal velocities of water drops. *J. Appl. Meteorol.*, **13,** 108–113

Bougeault, P., Binder, P., Buzzi, A., Dirks, R., Kuettner, J., Houze, R., Smith, R. B., Steinacker, R. and Volkert, H. 2001 The MAP Special Observing Period. *Bull. Am. Meteorol. Soc.*, **82,** 433–462

Bringi, V. N. and Chandrasekar, V. 2001 *Polarimetric Doppler weather radar principles and applications*. Cambridge University Press, Cambridge, UK

Campos, E. and Zawadzki, I. 2000 Instrumental uncertainties in Z–R relations. *J. Appl. Meteorol.*, **39,** 1088–1102

Doelling, I. G., Joss, J. and Riedl, J. 1998 Systematic variations of Z–R relationships from drop size distributions measured in northern Germany during seven years. *Atmos. Res.*, **47–48,** 635–649

Dotzek, N. and Beheng, K. D. 2001 The influence of deep convective motions on the variability of Z–R relations. *Atmos. Res.*, **59–60,** 15–39

Douglas, R. H. 1964 'Hail size distribution'. Pp. 146–149 in Proceedings of the eleventh radar weather conference, Boston, MA. American Meteorological Society, Boston, USA

Frei, C. and Schär, C. 1998 A precipitation climatology of the Alps from high-resolution rain-gauge observations. *Int. J. Climatol.*, **18,** 873–900

Folland, C. K. 1988 Numerical models of the rain-gauge exposure problem, field experiments and an improved collector design. *Q. J. R. Meteorol. Soc.*, **114,** 1485–1516

Germann, U. and Joss, J. 2002 Meso-beta profiles to extrapolate radar precipitation measurements above the Alps to the ground. *J. Appl. Meteorol.*, **41,** 542–557

Habib, E. and Krajewski, W. F. 2002 Uncertainty analysis of the TRMM ground validation radar-rainfall products: Application to the TEFLUN-B field campaign. *J. Appl. Meteorol.*, **41,** 558–572

Jameson, A. R. and Kostinski, A. B. 2001 What is a raindrop size distribution? *Bull. Am. Meteorol. Soc.*, **82,** 1169–1177

Joss, J. and Dyer, R. 1972 'Large errors involved in deducing drop-size distributions from Doppler radar data due to vertical air motion'. Pp. 179–180 in Preprints of the 15th radar meteorology conference, Champaign-Urbana, Illinois. American Meteorological Society, Boston, USA

Joss, J. and Gori, E. G. 1976 The parameterization of raindrop size distributions. *Riv. Ital. Geofis.*, **3,** 275–283

1978 Shapes of raindrop size distributions. *J. Appl. Meteorol.*, **7,** 1054–1061

Joss, J. and Lee, R. 1995 The application of radar–gauge comparisons to operational precipitation profile corrections. *J. Appl. Meteorol.*, **34,** 2612–2630

Joss, J. and Waldvogel, A. 1967 Ein Spektrograph für Niederschlagstropfen mit automatischer Auswertung. *Pure Appl. Geophys.*, **68,** 240–246

Joss, J., Schädler, B., Galli, G., Cavalli, R., Boscacci, M., Held, E., Della Bruna, G., Kappenberger, G., Nespor, V. and Spiess, R. 1998 *Operational use of radar for precipitation measurements in Switzerland.* vdf Hochschulverlag AG an der ETH Zürich, Switzerland

Kessler, E. 1969 *On the distribution and continuity of water substance in atmospheric circulation.* Meteorological Monographs, Vol. 10, No. 32. American Meteorological Society, Boston, USA

Kostinski, A. B. and Jameson, A. R. 1997 Fluctuation properties of precipitation. Part I: On deviations of single-size drop counts from the Poisson distribution. *J. Atmos. Sci.*, **54,** 2174–2186

Marshall, J. S. and Palmer, W. M. 1948 The distribution of raindrops with size. *J. Meteorol.*, **5,** 165–166

Rotunno, R. and Ferretti, R. 2003 Orographic effects on rainfall in MAP Cases IOP 2b and IOP 8. *Q. J. R. Meteorol. Soc.*, **129,** 373–390

Sekhon, R. S. and Srivastava, R. C. 1971 Doppler radar observations of drop-size distribution in a thunderstorm. *J. Atmos. Sci.*, **28,** 983–994

Sheppard, B. E. 1990 Effect of irregularities in the diameter classification of raindrops by the Joss–Waldvogel disdrometer. *J. Atmos. Oceanic Technol.*, **7,** 180–183

Sheppard, B. E. and Joe, P. 1994 Comparison of raindrop size distribution measurements by a Joss–Waldvogel disdrometer, a PMS 2DG spectrometer, and a POSS Doppler Radar. *J. Atmos. Oceanic. Technol.*, **11,** 874–887

Smith, P. L. and Joss, J. 1997 'Use of a fixed exponent in 'adjustable' Z–R relationships'. Pp. 254–255 in Preprints of the 28th conference on radar meteorology, Austin, TX. American Meteorological Society, Boston, USA

Smith, P. L., Myers, C. G. and Orville, H. D. 1975 Radar reflectivity factor calculations in numerical cloud models using bulk parameterization of precipitation. *J. Appl. Meteorol*., **14,** 1156–1165

Smith, P. L., Liu, Z. and Joss, J. 1993 A study of sampling variability effects in raindrop size observations. *J. Appl. Meteorol.*, **32,** 1259–1269

Steiner, M. and Smith, J. A. 2000 Reflectivity, rain rate, and kinetic energy flux relationships based on raindrop spectra. *J. Appl. Meteorol*., **39,** 1923–1940

Vignal, B., Galli, G., Joss, J. and Germann, U. 2000 Three methods to determine profiles of reflectivity from volumetric radar data to correct precipitation estimates. *J. Appl. Meteorol*., **39,** 1715–1726

Waldvogel, A. 1974 The N_o jump in raindrop spectra. *J. Atmos. Sci*., **31,** 1067–1078